Catalytic Photooxidation of Pentachlorophenol Using Semiconductor Nanoclusters

J. P. Wilcoxon†

Nanostructures and Advanced Materials Chemistry, Department 1152, Sandia National Laboratories, Albuquerque, New Mexico 87185-1421

Received: April 3, 2000; In Final Form: June 5, 2000

Pentachlorophenol (PCP) is a toxic chlorinated aromatic molecule widely used as a fungicide, a bactericide, and a wood preservation, and thus is ubiquitous in the environment. We report photooxidation of PCP using a variety of nanosize semiconductor metal oxides and sulfides in both aqueous and polar organic solvents and compare the photooxidation kinetics of these nanoclusters to widely studied bulk powders such as Degussa P25 TiO_2 and CdS. We study both the light- intensity dependence of PCP photooxidation for nanosize SnO_2 and the size dependence of PCP photooxidation for both nanosize SnO_2 and MoS_2. We find an extremely strong size dependence for the latter which we attribute to its size-dependent band gap and the associated change in redox potentials due to quantum confinement of the hole−electron pair. We show that nanosize MoS_2 with a diameter of $d = 3.0$ nm and an absorbance edge of ∼450 nm is a very effective photooxidation catalyst for complete PCP mineralization, even when using only visible-light irradiation.

I. Introduction

Contamination of sediments and aqueous water systems by halogenated organic compounds presents a serious environmental threat due to their toxicity and resistance to biodegradation. These chemicals are widely employed as pesticides, insecticides, and wood preservatives and thus are ubiquitous in the environment of both industrialized and agrarian nations. Even chemicals which have been banned for years, such as DDT and its analogues, still pose major environmental threats and, in fact, constitute the basis of several EPA superfund sites. A subgroup of these chemicals referred to as chlorinated aromatics includes chlorinated benzenes and biphenyls (PCBs), pentachlorophenol (PCP), and insecticides such as DDT.

PCP, the topic of this paper, is widely found in the environment, and it belongs to a family of chlorinated phenols that are among the most toxic chemicals known to man. In general, the more chlorines on the aromatic phenol ring the greater the biohazard. It has been postulated[1] that the widespread detection of PCP and its analogues in the environment may result from combustion, water treatment with chlorine in the presence of organic materials, and municipal sewage treatment plants and incinerators. Once discharged into the environment, these rather water- insoluble compounds, (10−20 ppm in water, typically), seep into the sediment of rivers, lakes, and other bodies of water and continually leach out into the water supply, eventually affecting the entire mammalian food chain.

Microbial degradation and naturally occurring hydrolysis of these compounds is a very slow process (e.g., for 4-cholorophenol at 9 °C the half-life is nearly 500 days).[2] Some direct photodegradation also occurs, although the limited optical absorbance of chlorinated aromatics above 350 nm in wavelength makes this process painfully slow. Sometimes this direct photolysis can actually lead to more toxic products (e.g., direct photolysis of PCP has been reported to lead to octachlorodibenzo-*p*-dioxin, an even more toxic species than its precursor).[3]

It is clear that more effective methods of treatment of these chlorinated aromatics must be sought. To this end, a few groups have been investigating photocatalytic oxidation of these compounds to form harmless CO_2 and HCl, a process referred to as total mineralization.[2−4] The semiconductor catalyst of choice in these studies has been TiO_2, a white, photostable, nontoxic powder, whose principal deficiency is an absorbance edge which starts at about 385 nm, allowing less than 3% utilization of the solar spectrum.

It would be a major boon to have a visible-light-absorbing semiconductor catalytic material available, which is also photostable and nontoxic. Such a photocatalyst would make it possible to exploit sunlight as the sole energy source required for detoxification. To this end we have employed our expertise in nanocluster synthesis and processing to make and purify nanoparticles of MoS_2, whose band-gap and absorbance edges can be adjusted by particle size on the basis of the quantum confinement of the hole−electron pair. In a recent paper we demonstrated the use of these new photocatalysts to destroy phenol, and demonstrated a strong effect of size or band gap on the rate of photooxidation.[5]

The question of the effect of catalyst size on the photocatalytic activity has not been investigated very much for nanosize materials, particularly those whose size is small enough to affect their electronic energy levels via quantum confinement. Farin and co-workers[5] investigated the photoactivity of colloidal TiO_2 for propene photohydrogenation and found that the rate increased ∼7-fold upon decreasing the colloid size from 16 to 8 nm. Since a 4-fold increase in surface area occurs over this size regime, their observed rate increase is mostly accounted for by this increase in surface area and is probably not due to changes in either surface morphology or electronic levels. (The Bohr diameter for which quantum confinement effects are expected to be important is significantly smaller than 8 nm for TiO_2). More recently, Korgel and Monbouquette[6] investigated photocatalyzed reduction of nitate ions in deaerated water using dispersed 2 nm CdS nanocrystals stabilized with organic ligands. They found a very strong size dependence—a 10% decrease of

† E-mail: jpwilco@sandia.gov.

10.1021/jp0012653 CCC: $19.00
Published on Web 07/19/2000

TABLE 1: Synthetic Details for Catalysts Used in Photooxidation Studies[a]

sample name	surfactant/ solvent	precursor/ concentration	sulfiding or hydrolysis agent	rate of mixing	pH (final)
SnO_2(d = 25 nm)	2-propanol	Sn(isopropoxide)/ 50 mg/mL	HCl@pH = 1.5	0.1 mL/min	2
SnO_2(d = 58 nm)	2-propanol	Sn(isopropoxide)/ 25 mg/mL	HCl@pH = 1.5	0.01 mL/min	2
TiO_2 #28(d = 20 nm)	2-propanol	Ti(isopropoxide)/ 50 mg/mL	HCl@pH = 1.5	0.1 mL/min	2
TiO_2 #10(d = 55 nm)	2-propanol	Ti(isopropoxide)/ 25 mg/mL	HCl@pH = 1.5	0.01 mL/min	2
MoS_2(d = 3.0)	DTAC(8%)/ c6OH(11%)/c8	$MoCl_4$/0.002 M	H_2S(0.01 M)	NA	NA
MoS_2(d = 4.5)	DTAB(8%)/ c6OH(11%)/c8	$MoCl_4$/0.002 M	H_2S(0.01 M)	NA	NA
MoS_2(d = 8−10)	DTAB((1%)/ c6OH(1.5%)/c8	$MoCl_4$/0.002 M	H_2S(0.01 M)	NA	NA

[a] DTAC = dodecyltrimethylammonium chloride (Fluka Chemicals, 99%); DTAB = dodecyltrimethylammonium bromide (Fluka Chemicals, 99%).

the nanocrystal size resulting in a 5-fold increase in the rate of reduction! However, a sacrificial electron donor, formate, had to be utilized to prevent photocorrosion of the nanoparticles and to allow the reduction to occur.

In this paper we investigate the photooxidation kinetics and products formed for a standard material, Degussa P25 TiO_2, as compared to nanosize TiO_2, SnO_2, and MoS_2. We examine the light-intensity dependence for nanosize, fully dispersed SnO_2 compared to a slurry of TiO_2 (Degussa) at the same concentration. We show that because of the intense multiple scattering observed in slurries compared to dispersion of nanocrystals it is necessary to study both systems in a light-intensity regime where the reaction kinetics are both first-order in PCP.

We study photooxidation by nanosize SnO_2 in aqueous systems and, for the first time, a system consisting almost entirely of a polar organic acetonitrile, and show that total PCP mineralization occurs even with severely limited oxygen and water concentrations. Furthermore, we show that while simple salts such as NaCl poison the activity of P25 TiO_2, certain cationic surfactants can actually enhance its activity.

To understand the effect of catalyst size on PCP photooxidation kinetics we investigated various sizes of nanosize SnO_2 and MoS_2. However, in the former case the two sizes studied were larger than the size at which quantum confinement effects would be expected to affect the electronic energy levels of the material. We found a negligible size dependence for nanosize SnO_2, a surprising result in view of the nearly 4-fold difference in the surface areas of the two samples investigated. For nanosize MoS_2, strong quantum confinement effects are present which lead to a shift of as much as 2 eV in the band gap compared to bulk MoS_2. This large energy shift is invoked to explain the enormous size-dependence of the observed PCP photooxidation kinetics using this catalyst. We find that d = 3.0 nm MoS_2 which has an absorbance edge near 450 nm can mineralize PCP at a rate exceeding even that of P25 TiO_2, even though only visible irradiation was employed in our MoS_2 studies while full Xe lamp illumination was used in the our studies of P25 TiO_2.

II. Materials Synthesis and Experimental Procedures

Synthesis. In a previous paper describing the photooxidation of phenol, we gave details concerning the synthesis of nanosize MoS_2.[7] The electronic and optical properties of this remarkable, structurally anisotropic, indirect band-gap semiconductor are discussed elsewhere.[8−10] Nanosize TiO_2 and SnO_2 were prepared by the controlled hydrolysis of the corresponding metal isopropoxide in 2-propanol, and this general procedure has been described extensively by others in the literature.[11,12] We modified this general, acid-catalyzed metal alkoxide hydrolysis procedure by employing an aqueous solution of HCl at pH ∼ 1.5 which was slowly injected using a programmable syringe pump (KD Scientific Co., model 100 pump) into a rapidly stirred titanium or tin isopropoxide (Aldrich Chemical) in 2-propanol solution. It was discovered that both the pH and rate of addition of acid catalyst could be used to control the final size. In general we found that pH ∼ 2 or less was required to ensure long term (i.e., weeks to months) colloidal stability against aggregation. The final (post-mix) ratio of water to 2-propanol volumes was 10:1 in each case. In general, using higher pH values and slower mixing of the two solutions gave rise to larger nanoclusters as determined after 24 h by dynamic light scattering (DLS). We were able to vary the size as measured by DLS from about 10 nm to 150−200 nm, but we were only interested in the 10−30 nm size regime for photocatalysis purposes. Table 1 gives further details of the nanocluster synthesis, nanocluster size, and physical properties.

Degussa P25 TiO_2 was purchased from Degussa Chemical Company and used as received by making a stock solution of 10 mg/mL TiO_2 in milli-Q (Millicore Corp.) water. This stock solution was diluted as appropriate to achieve the desired catalyst concentration. No buffers or salts were added unless otherwise noted to any of our powder slurries or nanocluster solutions. CdS powder, 99.9% pure, ALFA Chemicals, was similarly used as received and dissolved in milli-Q water to make a standard 10 mg/mL solution which was then diluted for use in our photoreactor. Other powders investigated were also metals grade, purchased from ALFA and then made into stock slurries at 10 mg/mL. These stock solutions were used to prepared either 1 mg/mL or 0.1 mg/mL slurries in milli-Q water.

Purification/Processing of the Nanocatalysts. The as-synthesized MoS_2 nanoclusters were purified by extraction from the nonpolar solution in which they were prepared, octane, into a water-miscible but octane-immiscible solvent, acetonitrile (ACN). The MoS_2 clusters in ACN were dried to a very small volume (e.g., ∼0.5 mL) by centrifugal evaporation (∼40× reduction in volume) using a Centrivap (Labconco Corp.) with a cold trap, and then these reduced volume samples were added to water to form the catalyst solution.

Removal of ions and excess surfactants and 2-propanol from the nanocluster solutions of MoS_2, TiO_2, and SnO_2 using the as-prepared solutions was achieved by dialysis using a 500 M.W. cutoff Spectra-Por (Spectrum Medical Industries, Inc.) dialysis membrane and dialysis against 1 L of milli-Q water with one

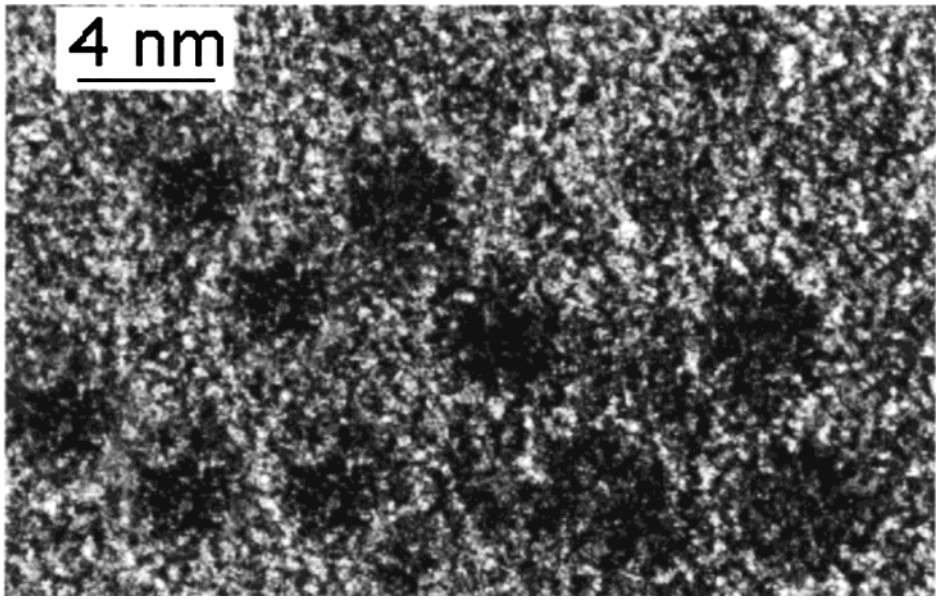

Figure 1. TEM of a field of $d = 3.0$ MoS_2 nanoclusters.

change over a 12−24 h period. Some aggregation as determined by DLS of the MoS_2 and TiO_2 nanoclusters occurred under these conditions, but the catalytic activity improved substantially. The nanocluster solutions were still visually transparent, temporally stable, and completely dispersed without agitation. All nanocluster catalyst solutions exhibited negligible light scattering in contrast to the control suspension of Degussa TiO_2 at a concentration of 0.1 mg/mL, which was milky-white and cloudy, and which exhibited intense multiple scattering. We note that the concentration of TiO_2 used in the present studies was about 16−20 times less than that used in most previous work, to try to minimize multiple scattering effects on the control catalyst. Even so, the intense multiple scattering characteristic of slurries of TiO_2 or CdS makes direct comparison of the quantum efficiency (Q.E.) of Degussa TiO_2 to the corresponding nanocluster solutions very difficult. Viable realistic approaches to address this issue have been discussed extensively in the literature.[11]

Catalyst Characterization. TEM and HRTEM were used to determine the nanocrystallinity of the materials, average cluster size, and polydispersity. The results were corroborated by use of DLS to measure the hydrodynamic diameter of the clusters in solution at the pH used for the photooxidation experiments. Except for nanosize TiO_2 this pH was ∼4.0 (the typical pH of our deionized milli-Q water) and the solution was not buffered, nor purged with any gases. It was necessary to keep the pH of the nanosize TiO_2 solutions at pH ∼ 2.0 to prevent aggregation. In the case of MoS_2, the clusters were so small that TEM gives a better measure of cluster size than DLS, but in the other cases the sizes reported were obtained from DLS which gives a better ensemble averaged size than TEM. Figure 1 shows a field of MoS_2 nanoclusters with an average size of $d = 3$ nm.

SAD has been used to determine that, for the case of nanoclusters of MoS_2, clusters large enough to give good electron diffraction (i.e., $d > 4.5$ nm), a crystal structure identical to bulk MoS_2 was observed.[8] Figure 2 shows XRD from a $d =$ 4.5 nm MoS_2 solution dried to form a powder compared to data from a commercial MoS_2 (99.7%, Alfa) powder obtained on the same instrument. Except for the broadening due to the small domain size, the structures are identical. Further details concerning the optical properties and physical characterization of MoS_2 are given elsewhere.[8]

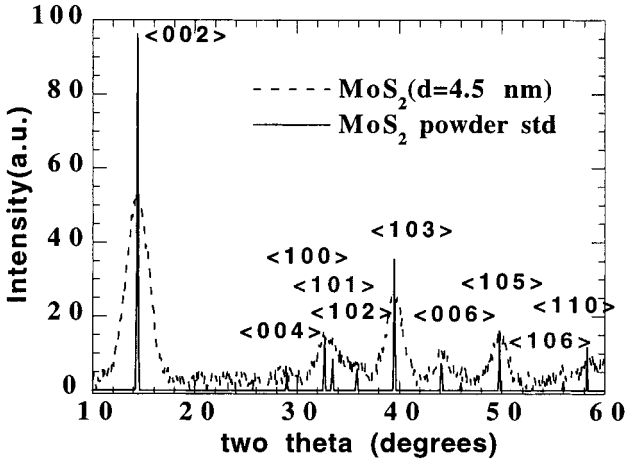

Figure 2. XRD from a $d = 4.5$ dried, nanocrystalline powder (dotted line) compared to a bulk powder of MoS_2 (solid line).

X-ray fluorescence (XRF) spectroscopy (Spectrace QuantX system) was used to determine the inorganic composition of the purified, processed nanocluster solutions as well as to obtain the absolute metal concentrations indicated in later figures. Using XRF analysis, it was also possible to determine approximately the metal-to-sulfur ratio despite the notoriously low (∼40 ppm) XRF sensitivity to low Z elements such as S, and to compare this to bulk powders of MoS_2. An example is shown in Figure 3, where bulk MoS_2 powder is compared to nanocluster solutions of purified MoS_2. In this figure we have indicated lines which arise from the cell windows and from the Ar present in the air environment. It was found that the ratio of Mo:S in our nanoclusters was ∼1:2.5 to 1:3, showing some excess sulfur on the nanocluster surface which could not be removed by our purification procedures. Later work using anion chromatography showed that this sulfur was in the form of adsorbed S^{-2} not SO_4^{-2}. This is fortunate since the latter oxidized form acts as the catalyst poison.

Catalyst Optical Properties. The optical absorbance properties of our nanocluster catalysts were determined using a Cary 2300 UV−visible−NIR spectrometer at the same concentrations used in the photooxidation studies. Slurries of Degussa TiO_2 in water were shaken and the spectrum rapidly obtained before

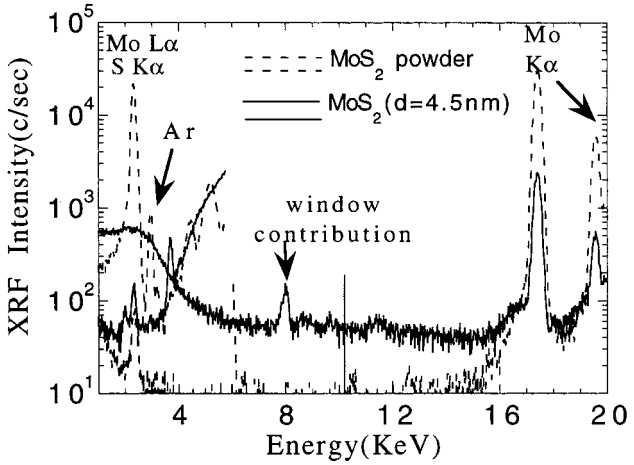

Figure 3. XRF lines from high purity bulk powder are co-plotted with purified nanosize MoS_2. Both Mo Kα and S Kα lines are shown.

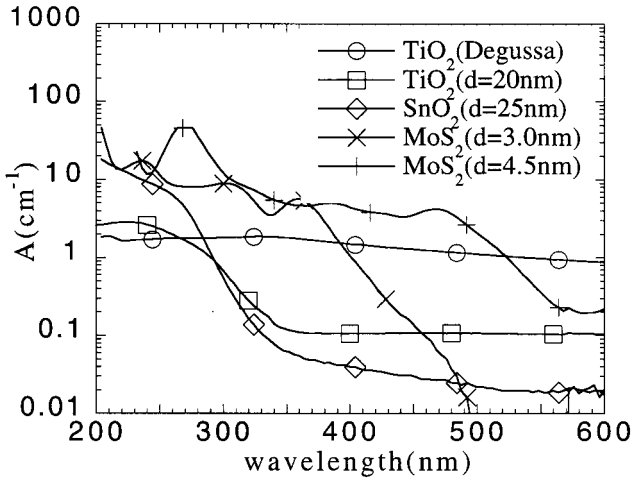

Figure 4. UV−visible absorbance spectra of nanocatalysts and control bulk powder (Degussa P25, TiO_2) are shown. All concentrations were 0.1 mg/mL.

powder settling occurred. The results of these absorbance measurements for nanosize TiO_2, SnO_2, MoS_2, and the Degussa TiO_2 slurries are shown in Figure 4. The strong multiple scattering of semi-opaque TiO_2 slurries even at 0.1 mg/mL in the 0.2 cm path length cell obscures the true band-edge absorbance of this material, which is clearly exhibited by the optically clear 20 nm diameter TiO_2 nanocluster solution. As can be observed in this figure, the TiO_2 slurry multiple scattering effectively enhances the absorbance probability of a photon in the relevant range of light output from our Xe arc lamp (300−400 nm) which corresponds to the actual TiO_2 absorbance (see the TiO_2 (d = 20 nm) nanocluster absorbance curve). Light scattering is negligible for SnO_2, MoS_2, and TiO_2 nanocluster solutions, and the absorbance curves of Figure 4 represent pure absorbance for these solutions.

PCP Optical Properties. To determine the optimum HPLC detector wavelengths to monitor the PCP concentration as a function of irradiation time, we first obtained the PCP absorbance spectrum at 10 ppm in water, methanol, and acetonitrile using our Cary 2300 spectrophotometer. These spectra are shown in Figure 5. Note that the PCP absorbance is solvent dependent. This fact is important because the chromatography was run in an isocratic 70:30 MeOH:H_2O ratio to optimize separation and peak shape, while still having an acceptably short run time for the metal oxide nanocatalysts. In the case of the MoS_2 nanoclusters the chromatography was performed in a

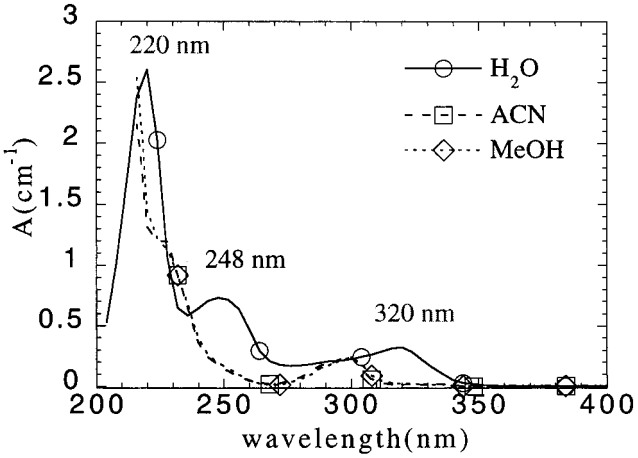

Figure 5. UV−visible absorbance spectra of PCP in three common HPLC solvents, water, methanol (MeOH), and acetonitrile (ACN).

solvent gradient from 70:30 ACN:H_2O to 100% ACN over 20 min time to give good elution peak shape of the nanoclusters themselves. We find that the PCP absorbance under the mixed organic:H_2O conditions most closely resembles the H_2O absorbance shown below so we chose to obtain PCP concentrations on the basis of the absorbance at 325, 250, and 215 nm.

Photooxidation Reactor. Our photooxidation reactor consists of a custom built (Ace Glassware Co.) cylindrical reactor with a flat glass base and an O-ring sealed quartz, Ace threaded window holder, with an aperture larger (∼3 cm) than our collimated Xe lamp output beam, (∼1.5 cm). The reactor has a total volume of about 60 mL, and we use 40 mL of liquid in all our reactions. The reactor has an O-ring sealed, Ace threaded, 45° sidearm for liquid- or gas-phase sampling through a septa, if desired, but in all the studies to be described we simply removed the O-ring plug and sampled 0.6 mL of the sample at various irradiation times for analysis. This aliquot was filtered using a Hewlett−Packard HPLC filter (0.45 micron, cellulose) to remove suspended catalysts into a standard 2 mL crimp-top HP HPLC vial for either HPLC or GC/MS analysis. We tested to make sure no PCP was being adsorbed onto the filter. This filter allowed the nanosize catalysts to pass through and so we could simultaneously do HPLC analysis of the MoS_2 nanocluster catalysts.

We used a commercial 400 W Xe arc lamp from Oriel. The output of this lamp is very close to that of the solar spectrum when combined with the 700 nm short-pass filter used. Overhead illumination of the cylindrical reactor is very advantageous since the flat-bottom geometry of our cell allows rapid magnetic stirring of the catalyst solution—a vital aspect affecting the photooxidation rate of the powder slurries used as control catalysts. This stirring is unimportant for the nanosize catalysts, but for consistency we maintained the same rate for these catalysts too. To study only visible-light photooxidation a 400 nm long-pass filter was also used to limit the incident irradiation wavelength, λ to 400 nm $< \lambda <$ 700 nm. The lamp light output is monitored continuously by a Newport research (Newport Corp., model 835) power meter with an IEEE-488 interface to a MacIntosh IIci computer, to track total irradiation time and any power variations. The incident power was measured using the 1 cm^2 size calibrated photodiode probe from Newport Research Corp. Neutral density filters on suprasil quartz substrates (Oriel Corp.) were used to attenuate the incident light by known amounts.

HPLC, GC/MS, and Cl Ion Analysis of PCP Photooxidation Kinetics. To study the rate of photooxidation of PCP

we used a HP 1050 high-pressure liquid chromatography (HPLC) system equipped with a photodiode array (PDA), a refractive index (RI), and a fluorescence (FL) detector(s). Unfortunately, the latter detector, though the ultimate in sensitivity for non-chlorinated aromatics like phenol, is nearly useless for PCP detection due to the quenching of the fluorescence by the chlorines on the aromatic ring of PCP. Nevertheless, we excited at 250 nm and detected fluorescence at 320 nm using this detector to detect any non-chlorinated aromatic byproducts at the ppb level that might be formed during the photooxidation process. The entire spectrum from 200 nm (the solvent cutoff) to 600 nm is available at each time point in the elution peak chromatogram, but for quantitation purposes we chose to monitor at the three broad main features in the PCP spectrum shown in Figure 5, 325, 250, and 215 nm. The latter wavelength gives the most sensitivity, while the former two can be used to avoid any detector saturation effects at high PCP concentrations and to check for consistency. Stock solutions of 10, 1, and 0.1 ppm PCP in milli-Q water were prepared, and a linear detector response over this concentration range was verified. A minimum sensitivity of about 0.02 ppm was determined for absorbance at 215 nm. This is significantly better sensitivity than we could achieve using our HP 5890/5972 GC/MS even using selective ion monitoring.

Obtaining acceptable peak elution symmetry and retention time stability from a highly chlorinated aromatic like PCP is a very challenging chromatography problem. We found that using an HP analytical ODS200 column (reverse phase c18 terminated silica, 200 mm (length) by 4.6 mm (diameter) with 5 mm particle packing and 120 Å pores), and running a 60:40 or 70:30 methanol (MeOH):H_2O mobile-phase mixture gave the best elution profiles, with good retention time stability over many runs. Various composition gradients of this mixture to 100% MeOH were also used to improve the separation if multiple organics were present. Using this solvent mixture it was also possible to detect the nanoclusters of MoS_2, but we found that acetonitrile (ACN) gave more reproducibility for the nanocluster peak shape and elution time so a 60:40 ACN:H_2O to 100% ACN was used in the MoS_2 nanocatalyst studies. This condition separates the nanoclusters, any surfactant, and PCP completely. We tried to use an independent column of the same type for the studies involving nanoclusters since some adsorption of the nanoclusters onto the column over many injections was found to alter the chromatographic elution behavior (i.e., peak shape, retention time) of the PCP, though not its quantitation (i.e., peak area). In all of our studies we inject 50 μL of the 600 μL sample taken at a given time point in the irradiation, and analyze the area under the elution peak at the three monitoring wavelengths, taking the average as the concentration of PCP at that point in time.

Generally, because of the low concentrations and limited solubility of PCP in water ($\sim$20 ppm), it is not possible to use gas chromatography/mass spectrocopy (GC/MS) to directly identify unknown photooxidation byproducts observed in HPLC using ion fragmentation patterns in MS, so we purchased several putative photooxidation intermediate candidates such as tetrachlorocatechol from Aldrich Chemicals and ran HPLC on these chemicals under identical chromatography conditions as used in the PCP photooxidation experiments. This allowed us to identify any possible intermediates via retention time alone. We also had the luxury of the complete absorbance spectrum of each elution peak to identify whether a compound observed was aromatic or not. Nevertheless, we were not able to identify all intermediates positively and we never observed tetrachlorocatecol, a logical intermediate to be formed by OH radical attack on a Cl on the PCP ring. However, our inability to identify most intermediates was not a major problem as all these compounds were eventually completely mineralized themselves. On the basis of the rate of appearance of these minor peaks compared to the rate of disappearance of the PCP peak, it was clear that these photooxidized compounds were not true intermediates on the pathway to complete mineralization, but rather, minor alternative photooxidation paths.

At the conclusion of several of the photooxidation reactions that were run long enough to achieve >99% disappearance of the PCP elution peak we used a Cl^- selective electrode to determine [Cl]. We were able to verify that the expected amount of free chloride was generated as calculated from the initial concentration of 10 ppm PCP, so complete detoxification was accomplished with the best nanosize photocatalysts using only visible illumination as well as with nanosize SnO_2 and Degussa TiO_2 using full (UV + visible) lamp illumination. Because of the small reactor volume and large Cl electrode size, it was not possible to follow the [Cl] in situ.

III. Experimental Results and Discussion

Direct Photolysis. It is interesting to compare the results of direct photolysis of PCP with that observed with Degussa TiO_2. In Figure 6a we show the absorbance at 215 nm, A(215 nm) vs elution time, t for different irradiation times using unfiltered Xe lamp illumination of PCP at 10 ppm in water. The products observed at the elution peaks of $t = 6.0$ min and $t = 3.27$ min were not observed in the catalytic photooxidation experiments. We found that measurements of the [Cl] using a Cl selective electrode at $t = 480$ min were consistent with nearly complete mineralization of the PCP under direct photolysis. This contrasts with some claims that only toxic intermediates such as octachlorodibenzo-*p*-dioxin are formed under direct photolysis.[14] The UV−visible spectrum at $t = 6.0$ is not consistent with such a product formation.

Pelizzetti et al.[15] studied the direct photolysis of PCP starting from an initial concentration of 12.5 ppm at pH = 3.0, and using a 1500 W Xe arc lamp with filters providing irradiation from 310 to 800 (conditions very similar to the present work except for the 3-fold increase in lamp intensity) and surprisingly observed a much slower rate of direct photolysis than we show in Figure 6a, even though their light intensity was more than 3-fold lamp greater than in the present work. This may be due to differences in reactor geometry.

Catalytic Photooxidation. The generally accepted description of the complete mineralization of PCP in water is

$$2HOC_6Cl_5\,(PCP) + 7O_2 = 4HCO_2H + 8CO_2 + 10HCl \quad (1)$$

In previous work,[16] other intermediates in the complete reaction 1 included p = cholinil ($C_6Cl_4(=O)_2$) or its reduced form. However, detection of this compound is difficult due to its low optical extinction coefficient in water. Also, this compound is reported to be unstable when stored in water and must be extracted into ether to allow detection by HPLC, so we did not expect to observe this compound. We also did not monitor the CO_2 or formic acid concentrations because of the limited reactor volume we employed. However, our [Cl] measurement at completion (i.e., >99.9% PCP removal) $t \sim 480$ min was consistent with the stoichiometry described in eq 1.

When Degussa TiO_2 is added to the water at a concentration of 0.1 mg/mL the absorbance at 215 nm (A(215 nm) chromatograms) shows different reaction byproducts than observed in

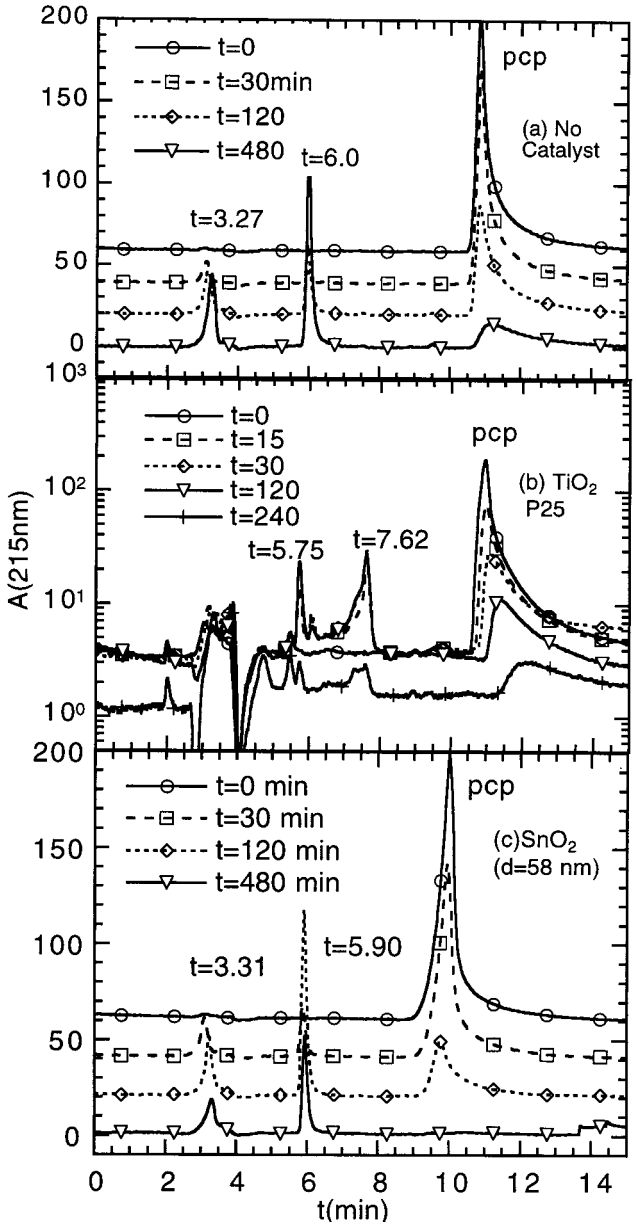

Figure 6. Photooxidation of PCP in water using a 400 W Xe arc lamp with the 300 nm < λ < 700 nm pass filters and measured incident intensity of $I_o = 250$ mW/cm^2 is followed by the absorbance monitored by a PDA at 215 nm, A(215 nm) vs elution time, t for three cases: (a) no catalyst, (b) Degussa TiO_2 (0.1 mg/mL) slurry, (c) nanosize (0.1 mg/mL) SnO_2. The chromatograms for different irradiation times are offset for clarity.

direct photolysis, Figure 6a. In fact, we observe different byproducts for each type of catalytic material we examined, TiO_2, SnO_2, and MoS_2.

In Figure 6b we show the results for catalytic photooxidation of PCP using Degussa P25 TiO_2 at a concentration of 0.1 mg/mL in milli-Q water. There is less buildup of intermediates than observed in the direct photolysis results of Figure 6a. The elution peaks at $t = 7.6$ min and $t = 5.8$ min are also destroyed more rapidly. Also, the photooxidation kinetics are significantly accelerated with the photocatalyst present.

Our observations of the increase in photooxidation rates with TiO_2 compared to direct photolysis are consistent with other work using Degussa P25.[1,16] Since our reactor geometry, initial concentrations, and catalyst concentrations are significantly different from previous work a direct comparison with these

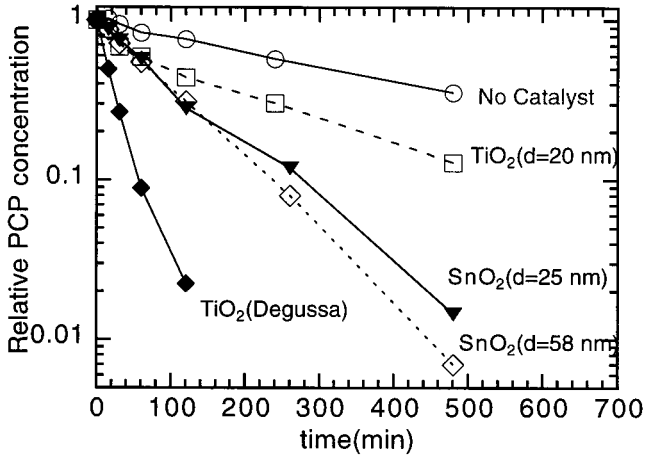

Figure 7. Normalized PCP concentration vs irradiation time using a 400 W Xe arc lamp with 300 nm < λ < 700 nm irradiation. Initial PCP concentration was 10 ppm in all cases, and the incident light intensity was 250 mW/cm^2.

other studies is difficult. However, our conditions are most similar to those employed by Mills et al.[16] in which a 450 W Xe arc lamp with IR cutoff filter was used and an initial concentration of 1.2 ppm was employed with 0.2 mg/mL of Degussa TiO_2 catalyst. They reported that complete mineralization was achieved under these conditions in about 3 h, consistent with our results taking into account our 8-fold larger concentration of PCP and 2-fold lesser catalyst concentration.

Our photocatalytic oxidation results using nanosize SnO_2 are shown in Figure 6c. (Bulk SnO_2 is nearly inactive for PCP photocatalysis). Here we observe breakdown products more similar to those of the direct photolysis results of Figure 6a, but with accelerated kinetics. No peak at $t = 7.6$ min is observed.

Nanosize SnO_2 has not been studied previously so these results cannot be compared directly to other work. However, the rate of disappearance is comparable to that observed from Degussa TiO_2. Since SnO_2 is cheaper than TiO_2, but is ineffective as a bulk photocatalyst, these results are encouraging as they provide evidence that a robust metal oxide material in nanosize form can be competitive with Degussa TiO_2 slurries.

By integrating the areas observed in Figure 6a−c and similar data collected for the other nanocluster catalysts studied, one can obtain the kinetics behavior shown in Figure 7. There are obviously dramatically different rates of photooxidation of PCP for these various metal oxides. As has been found by many others, Degussa P25 has remarkable catalytic activity compared to nanosize TiO_2 ($d = 20$ nm). Though initially Degussa TiO_2 is more active than the SnO_2 nanoclusters, they all reach >99% complete mineralization in ~8 h.

In previous work by Mills et al.,[16] the kinetics of photooxidation using Degussa P25 TiO_2 at 0.2 mg/mL was observed to be 0th order in [PCP] for [PCP] > 0.6 ppm. In contrast, Barbeni et al.[1] showed first-order behavior and an exponential decrease in [PCP] with irradiation time. Our results for both direct photolysis and to a lesser extent photocatalysis using Degussa TiO_2 and nanosize TiO_2 and SnO_2 also show an exponential decrease with time. However, the higher concentrations of TiO_2 used by previous workers and the resulting stronger multiple scattering may make previous determinations of the true kinetics ambiguous, as we show in our light- intensity studies.

The apparently faster rate of photooxidation using Degussa P25 TiO_2 compared to the other materials is partly due to its intense multiple scattering of light which serves to confine the incident photons more effectively in the reactor. In other words,

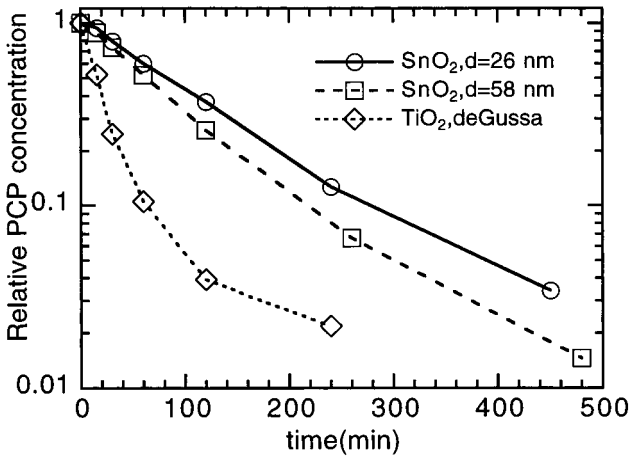

Figure 8. Relative concentration of PCP vs irradiation time for several nanocluster metal oxide catalysts using 10-fold attenuated incident light intensity $I = 0.1\ I_o = 25$ mW/cm^2.

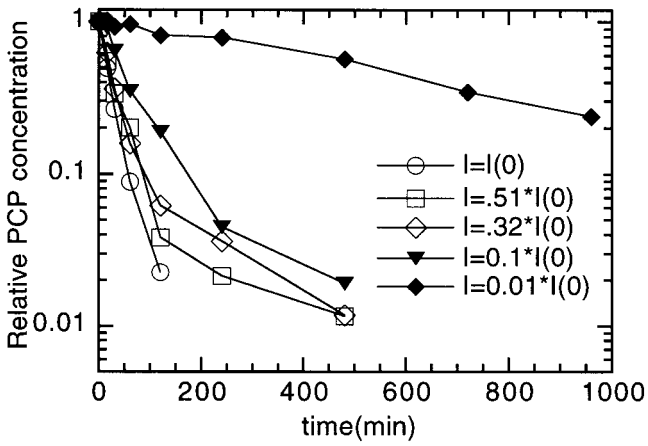

Figure 9. Relative PCP concentration (all initial concentrations were 10 ppm in water) vs irradiation time using a 400 W Xe arc lamp with the 300 nm $< \lambda <$ 700 nm pass filters and measured incident intensity of $I_o = 250$ mW/cm^2, and using Degussa P25 TiO_2 at 0.1 mg/mL.

its *effective* absorbance cross-section is larger. The other nanosize photocatalyst solutions, being transparent, are somewhat light-intensity limited at the 0.1 mg/mL or less nanocatalyst concentrations employed in these studies. This effect is illustrated most easily by comparison of the light-intensity dependence of Degussa TiO_2 vs nanosize SnO_2 as we do in the next section of this paper.

From Figure 7 we observe that the SnO_2 nanoclusters are less effective for photooxidation of the PCP than the P25 TiO_2 and, surprisingly, the smaller $d = 25$ nm SnO_2 nanoclusters are less efficient than the $d = 58$ nm SnO_2 nanoclusters despite their 4-fold advantage in geometric surface area. However, they are much more active than the nanosize TiO_2. We have also investigated the PCP photooxidation reaction in these systems with the incident intensity reduced 10-fold to see if photons are the "limiting reagent" in the nanocatalyst case but not in the TiO_2 slurry suspension case. This appears to be the case as shown in Figure 8. In the case of a slurry catalyst, the intense multiple scattering effectively increases the light path of the incident photons and thus their absorbance probability and so there are many more photons available than are needed for the reaction at the full lamp light intensity, 250 mW/cm^2. Thus, even when the photon intensity is reduced by an order of magnitude the slurry reaction does not slow proportionally, and the reaction kinetics for the slurry are not exponential under either of these irradiation conditions. However, under these irradiation conditions the nanocluster solutions are "starved" for photons and do slow in a proportional fashion and exhibit an exponential decrease in [PCP] with time.

From these studies one can conclude that it is necessary to study the strongly multiply scattering TiO_2 slurries at vastly reduced (10−100 fold) light intensities, to compare them to nanocluster dispersions at similar concentrations. For example, comparing Figures 7 and 8 we see that >99% photooxidation of PCP is reached in ~120 min for Degussa TiO_2 compared to four times as long for nanosize SnO_2, while, when the intensity is reduced 10-fold, Degussa TiO_2 takes ~240 min for >99% photooxidation while nanosize SnO_2 reaches this value in only twice the time.

We observe that there is little difference in photocatalytic oxidation activity for the two sizes of SnO_2 nanoclusters under these lower light level conditions. From this observation we can conclude that an increase in specific surface area alone is not enough to accelerate the kinetics for nanoclusters in this colloidal size range. This observation contrasts markedly from that described below for nanoclusters of MoS_2, where a very strong size dependence is observed due to quantum confinement effects.

Effect of Incident Light Intensity on Photooxidation Kinetics. Because of the strong light dependence demonstrated in Figures 7 and 8, we undertook a systematic investigation of the incident light-intensity dependence of nanosize SnO_2 compared to Degussa TiO_2 powder slurries. We did not attempt to make a similar comparison in the case of nanosize MoS_2 because of the significant difference in the absorbance edges of TiO_2 and nanosize MoS_2.

Figure 9 shows the change in photooxidation rate of PCP using a slurry of 0.1 mg/mL Degussa TiO_2 over a range of incident intensities of $I_o = 250$ mW/cm^2 (no light attenuation) to $I = 0.01I_o$. We were initially surprised by the very weak dependence of the kinetics on the incident intensity in the range $0.1I_o < I < I_o$. Apparently, due to extreme confinement of the light in the reactor due to multiple scattering from the slurry suspension, there are more than enough photons available so the reaction acts as if it is nearly zero-order in the light intensity. Only when the light intensity is reduced by about a factor of 100 does the kinetics of PCP photooxidation become exponential, as is the case with all the nanosize photocatalysts investigated. Therefore, one should really be comparing the PCP photooxidation kinetics for nanosize TiO_2 and SnO_2 to slurries of TiO_2 in this light-intensity regime. Unfortunately, this intensity is at least 2 orders of magnitude lower than has been previously investigated using Degussa TiO_2 and any organic.

Contrast the behavior shown in Figure 9 by the slurry suspension of TiO_2 to that exhibited by a nanocluster solution of SnO_2 using the same reactor geometry and irradiation conditions. The results of this experiment are shown in Figure 10. The same exponential PCP oxidation kinetics were observed for the nanosize TiO_2($d = 20$ nm), SnO_2($d = 25$ nm), SnO_2($d = 58$ nm), and MoS_2($d = 4.5$ nm). For each of the nonscattering nanocluster solutions we observe a rate that is roughly proportional to the incident light intensity, and the PCP oxidation kinetics appear exponential (i.e., first-order in [PCP]) over the entire light-intensity range investigated.

Other Powder Slurries. It has been demonstrated that certain materials, when prepared as semiconductor photoelectrodes, are effective photoelectrochemical catalysts.[17] The best-known example of this is RuO_2 which has been deposited on colloidal TiO_2 enhancing the rate of water photooxidation substantially.[17] We were interested in seeing if bulk powders of this and other

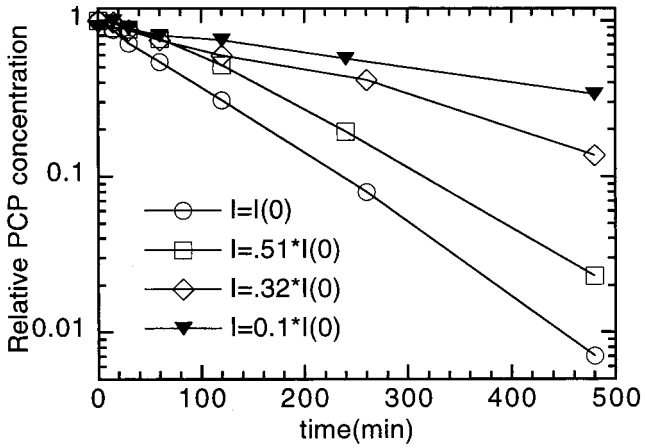

Figure 10. Relative PCP concentration (all initial concentrations were 10 ppm in water) vs irradiation time using a 400 W Xe arc lamp with the 300 nm < λ < 700 nm pass filters and a measured incident intensity of I_o = 250 mW/cm^2, and using nanosize, d = 26 nm SnO_2 at 0.1 mg/mL.

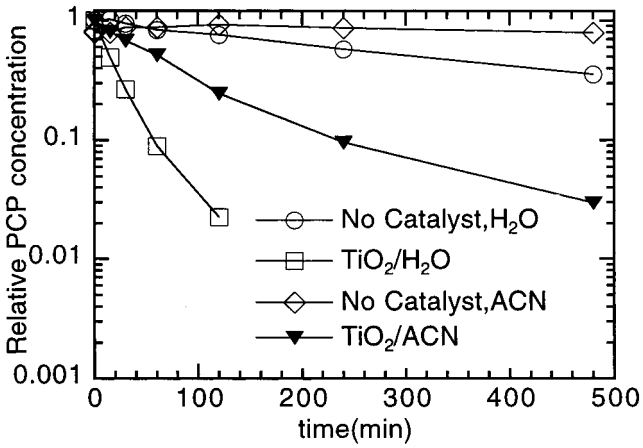

Figure 11. Relative PCP concentration (10 ppm at t = 0) vs irradiation time using a Xe arc lamp with I_o = 250 mW/cm^2 for no catalyst, and Degussa TiO_2 powder at 0.1 mg/mL in two solvents, milli-Q water and acetonitrile (ACN) containing 1 vol % water.

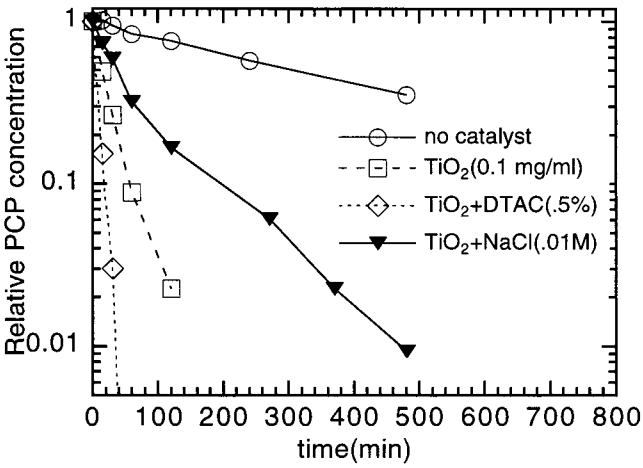

Figure 12. Relative PCP concentration (10 ppm initially in water) vs irradiation time. The effect of inorganic ions and surfactants on the photooxidation kinetics of PCP in water is shown.

similar materials would provide good photooxidation catalysts for organics such as PCP. Two of these materials, formulated as slurry suspensions in milli-Q water were studied. The powders were the highest grade purity available, obtained from ALFA Chemicals. The results were rather surprising, showing that these materials actually reduced the rate of normal photolysis and essentially acted as "anti-oxidation agents", preserving the PCP. We found this also to be true of bulk powders of MoS_2, WO_3, and SnO_2. The mechanism of this effect is quite mysterious, but does indicate that the presence of suspended, micron-size, inorganic materials may substantially decrease the rate of photooxidation of organic pollutants. This effect deserves more extensive examination, but does emphasize the remarkably rapid rates of photooxidation we observe in nanosize semiconductors as illustrated in Figure 10 . It is interesting to note that PtS_2 has the same layered hexagonal structure found in MoS_2, but in bulk form is very ineffective as a bulk photocatalyst as is bulk MoS_2 powder, probably due to having too narrow a band gap. As we will see, nanosize MoS_2 with its substantially wider gap is very effective as a photocatalyst.

Photooxidation of PCP in Polar, Nonaqueous Solvents. It has been postulated that photooxidation of organic materials using semiconductors in water requires the presence of OH radicals generated from the water to proceed at any appreciable rate.[15] Furthermore, many researchers deliberately aerate their photocatalyst suspensions in order to optimize the photooxidation process, and claims have been made numerous times that nearly total quenching of the photooxidation process occurs when inert gas purging is employed.[1] Thus, the use of aprotic organic solvents should cause a severe quenching of the photooxidation due both to the lack of OH radicals and reduced oxygen levels because of reduced gas solubility.

Figure 11 shows a study of the effect of solvent on the photooxidation of PCP both in direct photolysis (no catalyst) and using Degussa TiO_2 at 0.1 mg/mL. As observed in this figure, though the rate of photooxidation is 2−5× slower in ACN, photocatalysis does occur, indicating the mechanism for PCP photooxidation in water and in ACN is similar. This is verified by the presence of the same t = 7.6 min elution peak (see Figure 2) representing a photooxidation intermediate in the HPLC chromatogram for both solvents. As stated earlier this intermediate is not a catechol (i.e., the product of OH radical attack on a Cl on the aromatic ring). In ACN, it is a larger peak which is more slowly broken down when compared to water, however. This shows there are subtle differences in the photooxidation mechanism for the two solvents. The important conclusion from this experiment is that the presence of significant amounts of H_2O is not critical for the photooxidation of PCP. It would be interesting to extend these experiments to a wider range of organic chemicals, solvents, and photocatalysts to test the generality of our results.

Effect of Surfactants and Salts on PCP Photooxidation. In many real world situations, there are both multiple organic pollutants, inorganic salts, and even surfactants present in the water. Very little research is available in the literature comparing the effects of these complexities on the photooxidation kinetics, and nothing is known concerning their effects on PCP photooxidation. Thus, we examined separately the effect of a simple, common salt, NaCl, and a common type of organic, water-soluble surfactant, a quaternary ammonium salt, dodecyltrimethylammonium chloride (DTAC), on the photooxidation kinetics. We selected this surfactant for investigation since we use it to stabilize nanosize MoS_2 against aggregation, and because it has the common counterion, Cl, for comparison to NaCl, so we can separate out the effect of Cl from that of the organic dodecyltrimethylammonium entity.

The results of our investigations are summarized in Figure 12, for a single catalyst, Degussa P25 TiO_2 in water at 0.1 mg/mL under 300 nm < λ < 700 nm irradiation from our 400 W

Xe arc lamp. We first observe that even low levels of NaCl have a poisoning effect on the catalyst, though it is mild in this case. Similar observations have been made in field tests of TiO_2 where diionization of the aqueous waste stream have been found to be necessary.[19] In the laboratory, Barbeni et al.[1] reported no inhibition by NaCl at 1×10^{-3} M, so it appears that it is inhibitory only at the higher levels investigated here.

We expected the role of surfactants to be inhibitory—blocking access to surface sites on the semiconductor. However, our surprising observation is the significant acceleration of the photooxidation of PCP in the presence of the surfactant DTAC. We made similar observations of enhanced photooxidation rates in the case of nanosize MoS_2 and SnO_2. Clearly, the surfactant does not serve to block key surface sites as we expected. Instead it somehow aids the electron and/or hole transfer process. It is interesting to note that the use of a structurally similar surfactant, dodecyltrimethylammonium bromide (DTAB), also accelerates the photooxidation process, though not as much as DTAC, and that these observed increases in photooxidation rate are also seen using ACN as a solvent. So the counterion, Br or Cl, in the polar headgroup of the surfactant is important. It is important to note that the HPLC elution peak corresponding to the surfactant DTAC does not change in position or area, showing that these surfactants are robust compared to PCP during photooxidation. These types of multicomponent experiments are worth extending to other organic chemicals such as 4-chlorophenol, or phenol, due to the unexpected positive effects of the presence of these cationic surfactants.

In the studies of Korgel and Monbouquette[6] of the reduction of nitrate ion by nanosize CdS which was surface stabilized by charged organic thiols, they also found significant photocatalytic activity despite the strong surface binding of these ligands.

Photooxidation of PCP Using Nanosize MoS_2 and Visible Irradiation. In addition to the difficulties noted above in comparing transparent solutions of nanoclusters of TiO_2 or SnO_2 to strongly multiply scattering slurry suspensions of TiO_2, in the case of nanosize MoS_2 we also have qualitatively different absorbance characteristics between these oxide and sulfide materials, which render direct comparison of the photooxidation kinetics of our de facto standard, Degussa P25, to nanosize MoS_2 impossible. Basically, the problem is that under illumination using a 400 nm long-pass filter, TiO_2 has no activity, as expected, since its does not absorb light in the 400 nm $< \lambda <$ 700 nm region. So, for purposes of comparison to a bulk material suspension, we chose to use a metals grade CdS bulk powder (ALFA), whose absorbance onset of 525 nm is similar to that of nanosize MoS_2, and which, unlike TiO_2, does exhibit some photooxidation activity using 400 nm $< \lambda <$ 700 nm irradiation.

Figure 13 shows the relative PCP concentration vs time for two sizes of MoS_2 nanoclusters compared to CdS. The concentration of each MoS_2 solution as determined by XRF is shown in the figure, and it should be noted that due to some losses during the MoS_2 purification/dialysis, the concentrations are less than that of the CdS slurry suspensions. All other reaction conditions were identical.

Measurements of PCP concentration vs irradiation time by HPLC using a 70:30 ACN:H_2O to 100% ACN gradient elution allowed us to also determine the concentration of the surfactant-stabilized MoS_2 nanoclusters while we observed the destruction of the PCP. It was necessary to use ACN instead of MeOH as the organic component in these experiments to get good, reproducible HPLC of the nanoclusters. However, the HPLC peak symmetry of the PCP was not as good under these conditions, so we analyzed the irradiated samples using both

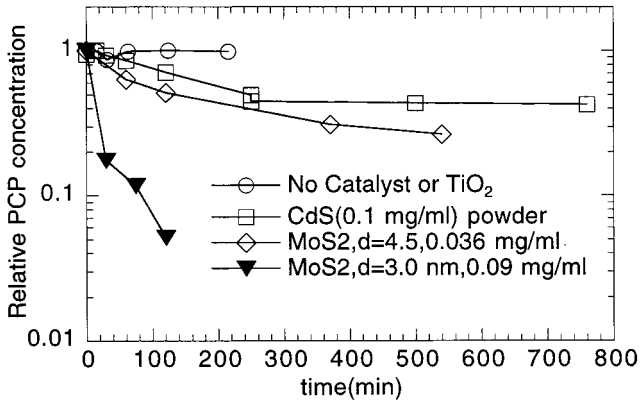

Figure 13. Relative PCP concentration in water vs irradiation time using a 400 W Xe arc with long- and short-pass filters allowing only 400 nm $< \lambda <$ 700 nm to reach the stirred solutions.

methods. We confirmed that the MoS_2 nanocluster elution peak area and corresponding optical spectrum of the nanoclusters under visible irradiation showed no changes with irradiation time, demonstrating that the MoS_2 nanoclusters were acting as true photocatalysts. There seemed to be no substantial improvement in the MoS_2 nanocluster photooxidation kinetics when full lamp (300 nm $< \lambda <$ 700 nm) was used. This result is not surprising given the relatively strong visible absorbance of both sizes of MoS_2 nanoclusters shown in Figure 3 coupled with the small lamp output below 400 nm.

Figure 13 demonstrates the dramatic effect of nanocluster size in the strong quantum confinement regime on PCP photooxidation kinetics. The change in size in this regime, it must be remembered, affects both the electronic valence and conduction band energy levels shifting them to more favorable values with decreasing size. Adding to the complexity of a direct comparison of the size effect in MoS_2 to that of control catalysts such as Degussa P25 TiO_2 is the larger surface area and change in relative number of Mo edge sites with decreasing size. The key observation, nevertheless, is that both $d = 4.5$ nm and $d = 3.0$ nm MoS_2 are substantially more active than CdS, though this slurry suspension effectively absorbs a substantially larger amount of incident light than the nearly transparent (i.e., nonscattering) MoS_2 solutions. It should also be noted, that though we did not perform a detailed study of the effect of nanocatalyst concentration on PCP photooxidation kinetics, this effect is weak (almost linear) for nanoclusters in the 0.01 to 0.1 mg/mL range due to the low PCP concentrations used (10 ppm). Our opinion is that the dramatic differences observed in the rates of photooxidation of PCP by $d = 3.0$ MoS_2 at 0.09 mg/mL and $d = 4.5$ mg/mL $d = 4.5$ MoS_2 at 0.036 mg/mL, is due primarily to the wider band gap of the former nanoclusters. This is because $d = 4.5$ nm MoS_2 with an absorbance onset of nearly 550 nm absorbs substantially more of the visible light than the $d = 3.0$ nm MoS_2 solution, with an absorbance onset of about 450 nm. It is worth noting that the PCP photooxidation kinetics curve terminates at $t = 120$ min for the case of $d = 3.0$ nm MoS_2 simply because the next point measured at $t = 240$ min showed no detectable PCP (i.e., less than 20 ppb)! By way of *very indirect* comparison, this is significantly better PCP photooxidation than is achieved using Degussa P25 TiO_2 and *full lamp irradiation* (i.e., 300 nm $< \lambda <$ 700 nm)!

Another strong argument favoring the effect of energy level shifts compared to a simple increase in surface area with decreasing size on the photooxidation kinetics is our observation of nearly identical photooxidation rates for $d = 26$ nm and $d = 58$ nm SnO_2 nanoclusters. These SnO_2 sizes are much too large

to affect valance and conduction band levels due to quantum confinement, yet the increase in specific surface area (total area/gram of catalyst) is very significant (almost 4×, about the same as that expected for the two sizes of much smaller MoS_2 nanoclusters!

We also examined our $d = 8-10$ nm MoS_2 nanoclusters employed in previous studies of phenol photooxidation[7] using visible irradiation and found very little activity, showing how important the quantum confinement and concomitant energy levels shifts are on the positive results of Figure 13. MoS_2 in the 8−10 nm size range absorbs intensely throughout the visible range 400 nm $< \lambda <$ 700 nm, but has a very small shift in the valence or conduction band levels relative to the bulk.[10] Although its specific surface area is admittedly considerably lower, (∼10×, this area reduction is not sufficient to explain its lack of activity.

IV. Conclusions

Using HPLC analysis we showed that the product intermediates in the photooxidation of PCP depend on whether a photocatalyst is used and also on the material type of the catalyst. Nanosize SnO_2, for example, gave different products than powders of Degussa TiO_2 or nanosize MoS_2.

We demonstrated a poisoning effect upon addition of a simple salt, NaCl, to slurries of TiO_2. More surprisingly, we observed that certain cationic surfactants actually enhance the activity of TiO_2 slurries and the degree of enhancement depended on the counterion, Cl or Br. Furthermore, HPLC showed that these cationic surfactants themselves were not photooxidized.

We also investigated the kinetics of PCP photooxidation as a function of light intensity comparing nanosize SnO_2 and TiO_2 to slurries of TiO_2. We showed that a fair comparison of the activity of these materials requires an investigation of the kinetics in light-intensity regimes where the reaction is first-order in PCP. For slurry systems, the intense multiple light scattering inherently increases the light collection efficiency of the reactor giving rise to an almost negligible dependence of the PCP photooxidation rate on the light intensity in the regime 25 mW/cm^2 $< I_o <$ 250 mW/cm^2. In this same intensity regime nanosize SnO_2 shows a proportional reduction with decreasing light intensity and first-order kinetics in [PCP], demonstrating that photons are a limiting "reagent" for these nanosize materials at the [PCP] typically found in the environment (1−10 ppm).

We made the first studies of PCP photooxidation using slurries of TiO_2 and nanosize SnO_2 in a polar organic solvent, ACN containing 1% H_2O. Surprisingly, we found significant, though reduced compared to pure H_2O, photocatalytic activity for both types of catalysts, despite the much lower O_2 and H_2O levels. This may indicate the role of hydroxyl radicals is not as critical in the total mineralization process as other researchers have suggested. It also indicates these photocatalysts will function adequately in aqueous systems containing a significant amount of miscible organic solvents.

In the case of nanosize SnO_2 we observed little or no size dependence of the photooxidation rate on size when comparing $d = 26$ nm to $d = 58$ nm SnO_2 colloids at the same mass concentration. Thus, it appears having larger available surface area, by itself, does not make this material more active.

The very strong MoS_2 size dependence we observe for this complex PCP photooxidation experiment is consistent with that observed for simpler photoredox reactions we have previously performed using time-resolved fluorescence to follow the electron transfer (E.T.) rates.[10] In these experiments we observed a dramatic reduction of E.T. rates to bipyridine and substituted bipyridine molecules as a function of increasing cluster size. It is also consistent with the strong size dependence we previously observed[7] in the visible-light-driven photocatalysis of phenol, where $d = 8-10$ nm MoS_2 had negligible activity while $d =$ 4.5 MoS_2 was active.

Acknowledgment. This work was supported jointly by the Division of Materials Sciences, Office of Basic Energy Sciences and the Energy Research/Environmental Management Program of the U.S. Department of Energy under contract DE-AC04-94AL8500. Sandia is a multiprogram laboratory operated by Sandia Corporation, a Lockheed−Martin Company, for the U.S. Department of Energy.

References and Notes

(1) Barbeni, M.; Pramauro, E.; Pelizzetti, E. *Chemosphere* **1985**, *14*, 195.
(2) Hoffmann, M. R.; Martin, S. T.; Choi, W.; Bahnemann, D. W. *Chem. Rev.* **1995**, *95*, 69.
(3) Mills, A.; Davies, R. H.; Worsley, D. *Chem. Soc. Rev.* **1993**, 417.
(4) Serpone, N.; Maruthamuthu, P.; Pickat, P.; Pelizzetti, E.; Hidaka, H. *J. Photochem. Photobiol., A: Chem.* **1995**, *85*, 247.
(5) Farin, D.; Kiwi, J.; Avnir, D. *J. Phys. Chem.*, **1989**, *98*, 5851.
(6) Korgel, B. A.; Monbouquette, H. G. *J. Phys. Chem. B* **1997**, *101*, 5010.
(7) Thurston, T. R.; Wilcoxon, J. P. *J. Phys. Chem.* **1998**, *103*, 11.
(8) Wilcoxon, J. P.; Newcomer, P.; Samara, G. A. *J. Appl. Phys.* **1997**, *81*, 7934.
(9) Tributsch, H. *Z. Naturforsch.* **1977**, *32a*, 972.
(10) Parsapour, F.; Kelley, D. F.; Craft, S.; Wilcoxon, J. P. *J. Chem. Phys.* **1996**, *104*, 1.
(11) Kiwi, J.; Borgarello, E.; Duonghong, D.; Gratzel, M. *Stud. Surf. Sci. Catal.* **1983**, *16*, 135.
(12) Jean, H.; Ring, T. A. *Langmuir* **1986**, *2*, 251.
(13) Serpone, N.; Terzian, R.; Lawless, D.; Kennipohl, P.; Sauve, G. *J. Photochem. Photobiol., A: Chem.* **1993**, *73*, 11.
(14) Plimmer, J. R.; Knliengebiel, U. I.; Crosby, D. G.; Wong, A. S. *Adv. Chem. Ser.* **1973**, *120*, 44.
(15) Pelizzetti, E.; Barbeni, M.; Pramauro, E.; Serpone, N.; Borgarello, E.; Jamieson, A.; Hidaka, H. *Chim. Ind.* **1985**, *67*, 623.
(16) Mills, G.; Hoffmann, M. R. *Environ. Sci. Technol.* **1993**, *27*, 1681.
(17) Hagfeldt, A.; Gratzel, M. *Chem. Rev.* **1995**, *95*, 49.
(18) Serpone, N. *Res. Chem. Intermed.* **1994**, *20*, 953.
(19) Crittenden, J. C.; Zhang, Y.; Hand, D. W.; Perram, D. L.; Marchard, E. G. *Water Environ. Res.* **1996**, *68* (3), 270.